Nozzle Exit Flow Profile Shaping for Jet Noise Reduction

R. W. Crouch* and C. L. Coughlin*
Boeing Commerical Airplane Company, Seattle, Wash.
and
G. C. Paynter†
Boeing Aerospace Company, Seattle, Wash.

Mixing of primary and secondary flows in a conventional turbofan engine provides a means of reducing jet noise. By shaping the nozzle exit velocity profile, noise reduction greater than that resulting from fully mixed flow has been achieved. In a static jet noise experiment, five primary flow nozzles were used with a common secondary nozzle to simulate exhaust flows of turbofan engines with bypass ratios from 1 to 5. Data are shown which relate jet noise to the location, extent, and magnitude of the peak velocity region. In general, minimum noise is obtained for inverted profiles where the outer area peak velocity is 5 to 15% greater than the reference uniformly mixed velocity, and the area of the peak velocity region is 40 to 50% of the total flow area. The inverted flow profiles produce noise characteristics similar to multielement jet suppressor nozzles, i.e., low frequencies are reduced and high frequencies are increased. It is shown that these spectral effects can be used to obtain a balanced noise signature.

Nomenclature

A = area
$\bar{A}$ = ratio of the nozzle exit area of a prescribed flow region relative to the fully mixed area
BPR = bypass ratio (ratio of secondary to primary mass flow rates)
D = diameter
M = Mach number
$\dot{m}$ = mass flow rate
OASPL = overall sound pressure level
OBSPL = octave band sound pressure level
P_t = thermodynamic total pressure
PNL = perceived noise level
PNLW = weighted perceived noise level, logarithmic PNL summation with angular weighting

$$= 10\log_{10}\left[\sum_{\theta=90^\circ}^{160^\circ,10^\circ}\left(\frac{10^{PNL(\theta)/10}}{\sin^2\theta}\right)\right]$$

PWL = sound power level
SPL = sound pressure level
T_t = thermodynamic total temperature
u = velocity
$\bar{u}$ = ratio of the nozzle exit velocity of a prescribed flow region relative to the fully mixed velocity
X = streamwise distance along jet axis downstream from nozzle exit
Y = distance perpendicular to jet axis
θ = acoustic angle relative to the "inlet" axis measured from the nozzle exit

Subscripts

mix = mixed flow properties
pri = primary flow properties
sec = secondary flow properties
1 = properties associated with the maximum velocity flow region at the nozzle exit plane
2 = properties associated with the minimum velocity flow region at the nozzle exit plane
3 = properties associated with the fully mixed flow region at the nozzle exit plane
1′ = properties associated with the secondary flow upstream of the nozzle exit in the mixing zone
2′ = properties associated with the primary flow upstream of the nozzle exit in the mixing zone
3′ = properties associated with the fully mixed flow upstream of the nozzle exit in the mixing zone

Presented as Paper 76-511 at the 3rd AIAA Aero-Acoustics Conference, Palo Alto, Calif., July 20-23, 1976; submitted Sept. 23, 1976; revision received May 19, 1977.
Index categories: Noise; Aeroacoustics.

*Specialist Engineer, Noise Technology Staff.
†Senior Specialist Engineer, Propulsion Technology Staff, Boeing Military Airplane Development.

Introduction

RECENT DOT/SST Phase II Jet Noise Suppression Program results[1] had shown that supersonic jet noise generation can be related to the shape or distribution of the nozzle exit flow velocity. These results suggested that nozzle exit velocity profile shaping also could be applied to other flow systems to obtain similar reductions in noise. An experiment was conducted to verify the profile shaping concept for subsonic/transonic jets. These data are now available to be used as a design guide for application of the profile shaping concept.

In many representative turbofan engine installations, the fan and primary flow streams are allowed to mix to some extent before passing through the nozzle. The amount of internal mixing which occurs and the radial and circumferential distributions of velocity at the nozzle exit plane are functions of the length of the mixing region and the way in which the fan and primary streams are brought into contact. Figure 1a illustrates a coannular nozzle installation in which the fan and primary flows come into contact at the nozzle exit plane without any internal mixing. Figure 1b illustrates the use of a lobed internal mixer to achieve mixed nozzle exit flow. Figure 1c illustrates the use of a lobed‡ internal mixer to achieve a partially mixed or shaped nozzle exit flow. In this case, tailpipe length, the shape and number of mixer lobes, and the radial and circumferential distributions of flow direction at the mixer exit plane are used to control velocity distribution at the nozzle exit.

In the present experiment, there was no circumferential distortion at the nozzle exit plane. Coannular coplanar

‡A lobed mixing device is used here only for purposes of illustration. Many other devices for achieving and controlling the internal mixing to shape the nozzle exit velocity distribution are possible.

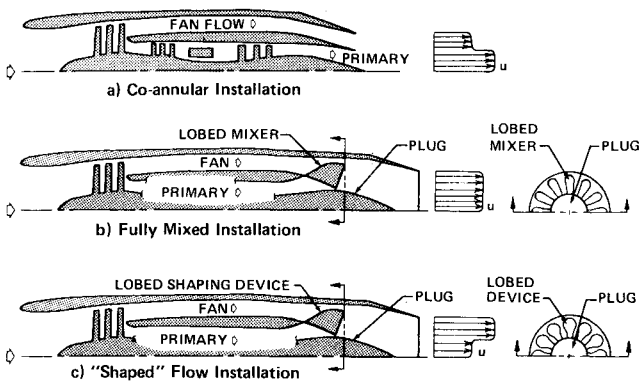

Fig. 1 Examples of profile shaping systems on turbofan engines.

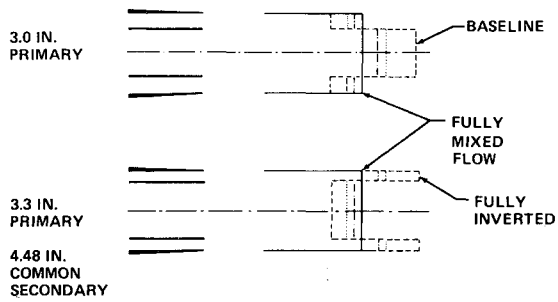

Fig. 2 Idealized velocity profiles for a typical run series.

nozzles were used as shown schematically in Fig. 2 to investigate the effects of radial shaping of the nozzle exit flow on jet noise characteristics. Various combinations of coannular primary and secondary nozzles were used to represent nozzle exit velocity profile shapes ranging from unmixed to fully mixed to fully inverted. The two fundamental parameters during this profile shaping process are velocity ratio and area ratio. Velocity ratio $\bar{u}_1$ is defined as the ratio of the maximum velocity to the fully mixed flow velocity. It is important to note that in the transition from baseline to inverted flow, the size of the primary nozzle changes for the fully inverted case, in order to conserve total energy and mass flow by maintaining constant area ratio where area ratio $\bar{A}_1$ is defined as the ratio of the nozzle exit area of the maximum velocity region to the fully mixed velocity area. (Total momentum is also approximately constant for the changes in profiles as explained in the appendix.) Gas properties in the primary and secondary streams were controlled independently to represent a range of turbofan engines.

One of the specific goals of this experiment was to determine whether profile shaping could be used to obtain noise reduction for a conventional turbofan flow system greater than that achieved by complete mixing. The acoustic effects of the profile shaping experiment are summarized in Fig. 3.

Three flows are considered: baseline, mixed, and inverted. The inverted secondary flow has the same peak velocity as the baseline primary flow but less area (part of the secondary gas has been sliced off from the inside and mixed with the primary). The parameter PNLW is a summation of the PNL's with an angular weighting that is the same as that used implicitly in the computation of airplane flyover effective perceived noise level. It provides a convenient measure of the duration effect between two noise signatures. It is observed in Fig. 3 that inverted flow provides a PNLW reduction of 1.7 PNdB beyond fully mixed. The duration weighted PNL directivity shows that the mixed flow peak is at 150°. The noy level spectrum at this angle shows that low frequencies are dominating the PNL for the mixed flow [noy level = $33.2 \log_{10}$ (noy value) + 40]. As will be shown, flow inversion produces acoustic effects similar to multielement nozzles, i.e., low

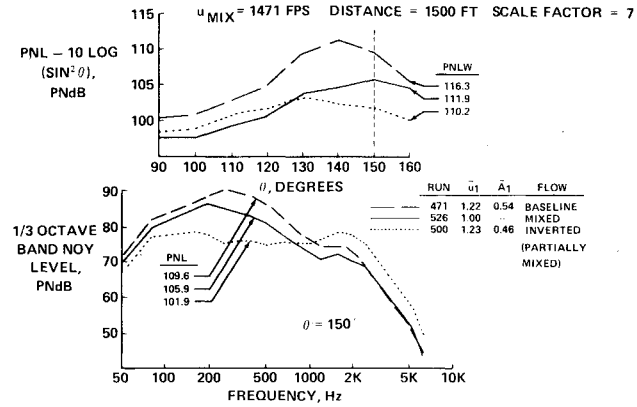

Fig. 3 Profile shaping for balanced noise characteristics.

frequencies are reduced and high frequencies are increased. In this case, these effects of flow inversion produce a balanced noise signature. The duration weighted PNL directivity and the noy spectra at peak angle are both nearly constant with angle and frequency, respectively. This illustrates the most important aspect of profile shaping – the potential for balanced noise characteristics.

The following sections quantify acoustic sensitivity to the following profile shaping parameters: velocity ratio, area ratio, and mixed velocity (throttle effect). The results are presented separately in physical units and subjective units. The practical considerations for applying profile shaping for jet noise reduction also are addressed. These include relative velocity effects, circumferential profile distortion, the potential performance improvement because of associated internal thermodynamic mixing, and a survey of methods of obtaining profile control such as internal forced mixer designs or engine cycle selections.

Experimental Arrangement

The profile shaping experiment was conducted at Boeing's Wall Isolation Facility located at North Boeing Field in Seattle, Wash. This facility is described in detail in Ref. 2. Coplanar dual flow was supplied to axisymmetric nozzle hardware by two independent airflow systems equipped with individual burners which could produce air temperatures from 430°F to over 1000°F. A heat exchanger was also available which lowered temperatures to 130°F. Primary and secondary airflow rates were measured upstream of the burner section with 3.1485-in.- and 3.000-in.-diam ASME flow meters, respectively. Five primary nozzles were tested with a common secondary nozzle in order to study area ratios ($\bar{A}_1$) from 0.28 to 0.54. Nominal diameters were 2.35, 3.0, 3.3, 3.6, and 3.8 in. for the primary nozzle and 4.48 in. for the secondary nozzle. Prior to acoustic testing, nozzle exit pressure and temperature profile plots for a range of conditions were measured to insure that the flow was symmetric and free of hotspots.

The far-field acoustic array consisted of 8 B&K 4135 ¼-in. microphones located on a vertical boom in a 25-ft polar arc from the nozzle exit. Free-field data were obtained with this arrangement. Microphones were positioned along the boom at 10° intervals from 90° to 160°, measured from the upstream flow direction.

The test matrix was arranged as follows: the 3.3, 3.0, and 2.35 in. primary nozzles were used with the 4.48 in. secondary nozzle to define three baseline flow systems corresponding to low, intermediate, and high bypass ratio turbofan flows ($\bar{A}_1$ = 0.54, 0.46, and 0.28 and BPR = 1.0, 1.6, and 5.0, respectively). The low and intermediate bypass ratio systems also were tested at three velocity regimes to simulate variations of engine power setting (throttle effect). Various degrees of exit flow profile shaping then were applied to these baseline flow systems through use of all five primary nozzles to generate

Table 1 Measured flow conditions[a]

DATA SET 1			Primary			Secondary		
RUN	$\bar{u}_1$	$\bar{A}_1$	$\dot{m}$	T_t	u	$\dot{m}$	T_t	u
526	1.00	–	4.49	600	1471	2.47	595	1465
486	1.05	0.54	3.78	700	1538	3.25	480	1382
476	1.09		3.60	805	1609	3.40	370	1300
481	1.14		3.42	925	1680	3.54	290	1235
471	1.22		3.49	1020	1794	3.72	200	1158*
420	1.04	0.46	3.09	695	1536	3.94	505	1397
425	1.09		2.96	805	1610	4.07	440	1346
415	1.15		2.85	920	1685	4.20	360	1290
410	1.23		2.65	1125	1804	4.36	285	1226
451	1.04	0.54	3.39	485	1381	3.64	695	1530
441	1.14		3.76	290	1232	3.35	920	1683
436	1.23		3.82	210	1167	3.53	1025	1805
515	1.05	0.46	4.11	510	1405	2.95	705	1543
510	1.10		4.27	430	1346	2.85	810	1612
500	1.23		4.64	275	1225	2.55	1125	1806
551	1.05	0.35	4.47	535	1420	2.50	700	1538
546	1.10		4.57	470	1375	2.46	805	1619
541	1.14		5.02	450	1357	2.15	920	1680
536	1.23		5.03	375	1271	2.14	1135	1810
DATA SET 2								
RUN	$\bar{u}_1$	$\bar{A}_1$	$\dot{m}$	T_t	u	$\dot{m}$	T_t	u
696	1.00	–	4.06	520	1317	2.47	515	1322
670	1.05	0.54	3.49	620	1388	3.04	400	1237
665	1.10		3.31	715	1446	3.21	310	1169
651	1.15		3.22	825	1516	3.36	235	1117
646	1.21		3.20	915	1602	3.50	180	1079*
586	1.10	0.46	2.74	715	1447	3.83	370	1216
581	1.15		2.61	825	1517	3.94	300	1158
576	1.21		2.49	970	1600	4.15	210	1090
611	1.05	0.54	3.21	410	1247	3.37	615	1383
606	1.10		3.34	310	1167	3.29	715	1451
601	1.14		3.60	240	1116	3.07	825	1509
596	1.21		3.71	180	1081	3.15	910	1596
691	1.05	0.46	3.84	435	1259	2.77	620	1385
681	1.15		4.11	295	1158	2.57	825	1516
676	1.22		4.35	215	1099	2.42	980	1605
735	1.05	0.35	4.39	470	1285	2.18	625	1384
730	1.10		4.33	420	1197	2.09	720	1449
725	1.15		4.73	370	1216	2.05	825	1520
721	1.21		4.85	320	1168	1.89	970	1595
DATA SET 3								
RUN	$\bar{u}_1$	$\bar{A}_1$	$\dot{m}$	T_t	u	$\dot{m}$	T_t	u
745	1.00	–	2.50	410	1051	3.01	415	1059
839	1.06	0.54	2.96	505	1124	2.59	315	1002
820	1.11		2.83	595	1173	2.72	225	939
815	1.16		2.73	695	1231	2.85	155	893
810	1.23		2.62	805	1296	2.96	135	899*
770	1.06	0.46	2.44	510	1120	3.05	335	999
755	1.16		2.20	695	1224	3.39	220	938
750	1.23		2.10	820	1296	3.46	160	890
795	1.06	0.54	2.63	335	1012	2.85	510	1119
785	1.16		3.01	155	893	2.63	695	1224
780	1.22		3.21	145	904	2.51	805	1290
855	1.11	0.46	3.33	285	981	2.28	595	1171
850	1.16		3.50	210	932	2.17	700	1225
845	1.22		3.64	155	890	2.05	825	1290
890	1.06	0.35	3.90	360	1039	1.86	505	1120
884	1.11		3.94	310	1000	1.76	595	1169
879	1.16		3.97	290	986	1.71	695	1227
870	1.22		4.10	245	954	1.64	820	1291

[a] T_t, °F; u, fps; $\dot{m}$, lb/sec; * = baseline flow systems.

seven sets of data. Only the low bypass ratio data will be discussed in detail in the following sections. The intermediate bypass ratio results are very similar to the low bypass ratio results, whereas the high bypass ratio data exhibited negligible profile shaping effects. The general procedure for calculating profile shaping flow conditions is presented in the appendix. Also, the measured flow conditions for the low bypass ratio data sets are tabulated in Table 1 (nominal area ratios are shown). Each data set is for approximately constant thrust conditions within each set. Sets 2 and 3 are at nominal 85% and 56% of the thrust conditions of set 1.

Results and Discussion

Acoustic Power Levels

Acoustic power is used to determine the effect of profile shaping on source strength. Acoustic power changes also provide an efficient means of relating noise changes to changes in the flow system. The power levels in this section correspond to the total acoustic energy radiated into the aft hemisphere with the exception of a 15° cone around the jet axis. Losses caused by atmospheric absorption were added to the measured data using Ref. 3 with required extrapolations for frequencies above 10 KHz. Frequencies below 400 Hz and above 40 KHz were not used in order to minimize the effects

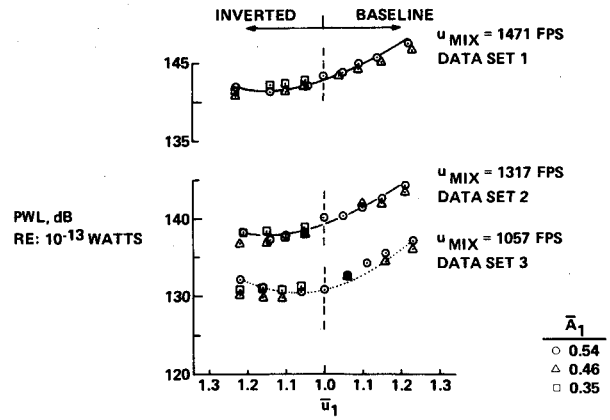

Fig. 4 Effect of profile shaping on power level.

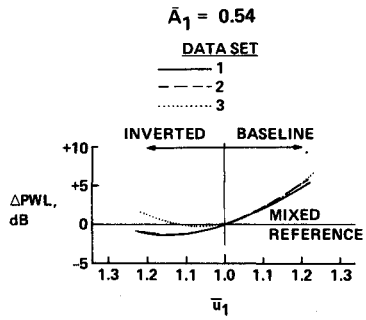

Fig. 5 Power level sensitivity to velocity regime.

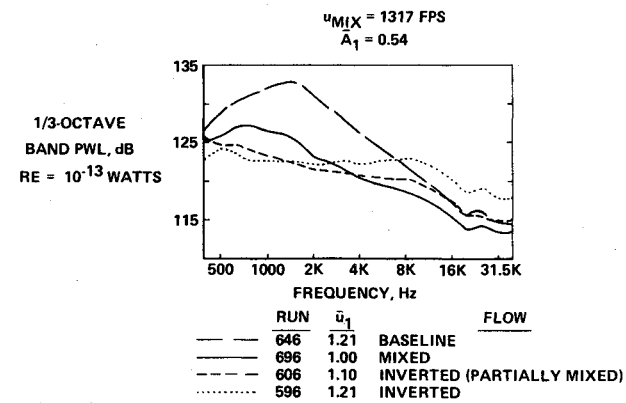

Fig. 6 Effect of inverted flow velocity on power spectra.

of burner noise and uncertainty in ultrasonic atmospheric absorptions.

The effect of profile shaping on total power level is shown in Fig. 4 for the low (BPR 1.0) bypass ratio system. The corresponding baseline area ratio is 0.54. Curves are drawn through data with this area ratio in order to isolate the effect of velocity ratio. Three velocity regimes are shown for each system. Power level reductions of almost 3 dB for inverted-type flows are shown relative to complete mixing. In general, minimum noise is obtained for inverted flows with a velocity ratio between 1.05 and 1.15. Area ratio has two effects. Area ratio 0.46 flows consistently have lower noise levels than area ratio 0.54 or 0.35 flows, which suggests that there is an optimum area ratio as well as velocity ratio for minimum noise. Also, as area ratio decreases, there is an increase in the velocity ratio that produces minimum noise. The fixed area ratio curve for each velocity regime has been crossplotted in Fig. 5 to show that inverted profiles produce greater reductions in source strength for higher-velocity flow systems.

The effect of inverted flow velocity on power spectra is shown in Fig. 6. In general, there is a reduction of low-

frequency noise and an increase in high-frequency noise for inverted flows relative to uniform fully mixed flows. The low-frequency reductions are consistent with the reduced downstream velocities produced by an inverted exit profile which promotes more rapid mixing. The increase in high-frequency noise is associated with an increase in shear between the secondary flow and ambient air. It is noteworthy that significant reductions in fully inverted high-frequency noise can be obtained for very slight loss in low-frequency suppression by partial mixing to reduce the peak velocity at the exit (e.g., run 606 vs run 596). These characteristics are similar to those exhibited by multielement jet suppressor nozzles. This behavior can be used to attain reductions in perceived noise levels.

The effect of inverted flow area ratio on power spectra is more subtle than the effect of velocity ratio. Power spectra for three inverted flows with the same secondary velocity are shown in Fig. 7. The fully inverted area ratio is 0.54. The other two area ratios represent slicing off secondary flow from the inside and mixing with the primary flow. An analytical flow program developed at Boeing[4] was used to understand better the noise results. Measured flow conditions at the nozzle exit were input to the flow program for the calculation of downstream profile development as shown in Fig. 8. All inverted flows have approximately the same initial peak velocity which is 300 fps higher than the reference fully mixed velocity. At downstream regions, velocities are lower than those obtained with the mixed flow system. This is consistent with the increase in high-frequency and decrease in low-frequency noise for inverted flows relative to complete mixing as previously discussed. In addition, for the three inverted flow area ratios compared in Figs. 7 and 8, the following correlations are observed. The fully inverted 0.54 area ratio flow produces the highest noise levels in the intermediate frequency portion of the spectra, which corresponds to the highest peak velocity from 1 to 4 diameters downstream. The 0.35 area ratio flow produces the highest noise levels in the low frequencies which corresponds to the highest peak velocity at diameters greater than 4. All three flow systems produce nearly the same high-frequency noise levels (16 KHz), which corresponds to the same initial peak velocity at the exit. It is not clear why the 0.46 area ratio flow produces the lowest noise at all frequencies, although it does provide the lowest peak velocity over a substantial axial distance.

Sound Pressure Levels

The amount of jet noise reduction available through profile shaping depends to a great extent upon the application. Perceived noise levels (PNL) often are used to define noise levels in the vicinity of airports. However, reductions in overall sound pressure levels (OASPL) may be more meaningful for applications where high-frequency energy can be attenuated greatly such as inside of dwellings and at areas of the community farther from the airport. The next section will address the effects of profile shaping on perceived noise. This section will evaluate the changes in OASPL with profile shaping and also present some typical spectra.

The effect of profile shaping on peak OASPL is shown in Fig. 9. These data correspond to the same flow systems previously shown in Fig. 4 in terms of acoustic power levels. The data here have been scaled using the indicated scale factor and extrapolated to 1500-ft distance at standard day conditions of 77°F and 70% relative humidity. Peak OASPL reductions of up to 4 dB for inverted-type flows are shown relative to complete mixing. General trends are the same as for power level changes. Minimum noise is obtained for inverted flows with a velocity ratio between 1.05 and 1.15, and area ratio 0.46 flows consistently produce lower noise levels than area ratio 0.54 or 0.35 flows. The fixed area ratio curves for each velocity regime are crossplotted in Fig. 10 to

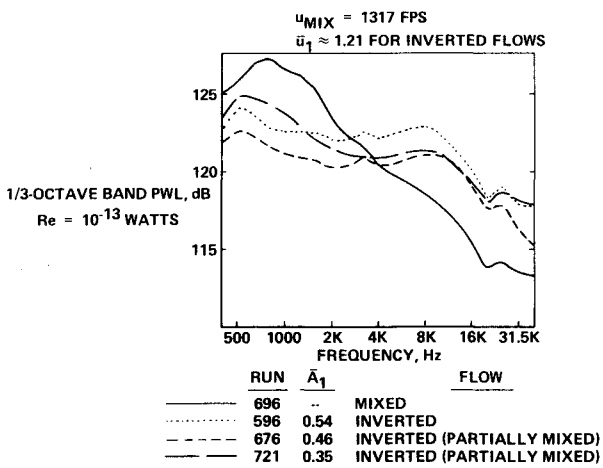

Fig. 7 Effect of inverted flow area ratio on power spectra.

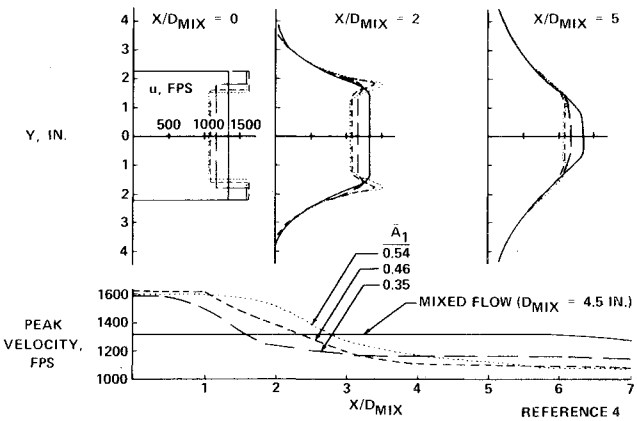

Fig. 8 Calculated flow profile development for inverted flow area ratio variation.

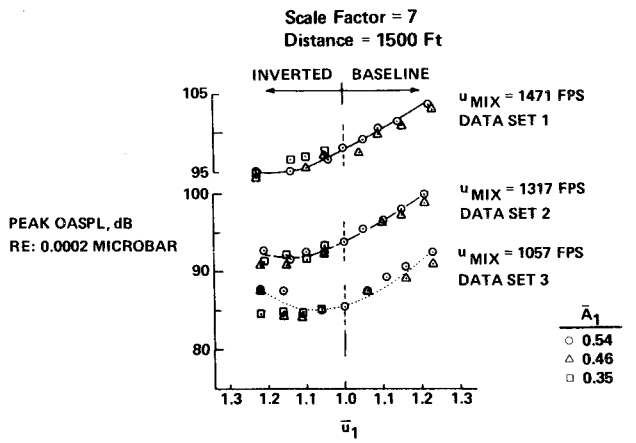

Fig. 9 Effect of profile shaping on peak OASPL.

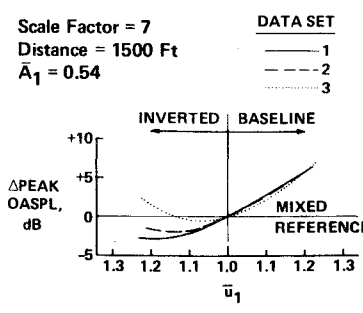

Fig. 10 Peak OASPL sensitivity to velocity regime.

show that inverted profiles produce greater reductions in peak OASPL for higher velocity flow systems. Also, there is a trend of minimum noise being obtained at higher velocity ratios for higher velocity flow systems.

The effect of inverted flow velocity ratio on OASPL directivity is shown in Fig. 11. Greatest noise reductions are obtained at large angles for inverted flows relative to complete mixing. It is observed that increases in noise can occur at forward angles. This increase is sensitive to the velocity ratio of the inverted flow. These directivity effects are related to the spectral changes as shown in Fig. 12 where the changes in low- and high-frequency levels are compared for the flow systems of Fig. 11. Flow inversion produces a uniform increase in high-frequency noise at all angles. The magnitude of this increase is strongly dependent on velocity ratio. In contrast, a decrease in low-frequency energy is observed primarily at the aft angles and the magnitude of this reduction is a weak function of velocity ratio.

The effect of inverted flow area ratio on SPL directivity is shown in Fig. 13 for the 200-Hz and 2000-Hz bands. Changes in high-frequency noise are much less sensitive to area ratio than velocity ratio. Some stratification of low-frequency levels is evident with minimum noise occurring for the area ratio 0.46 flow at all angles.

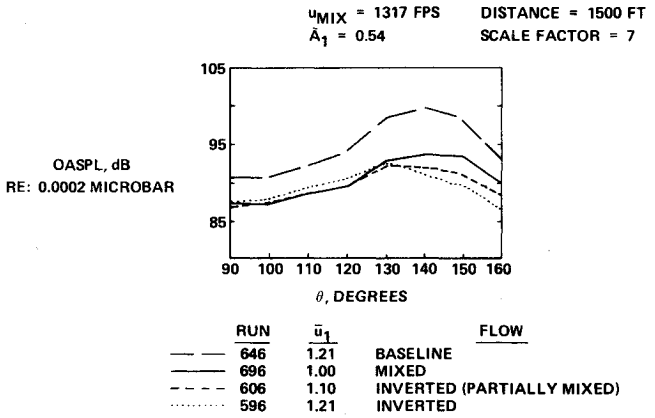

Fig. 11 Effect of inverted flow velocity on OASPL directivity.

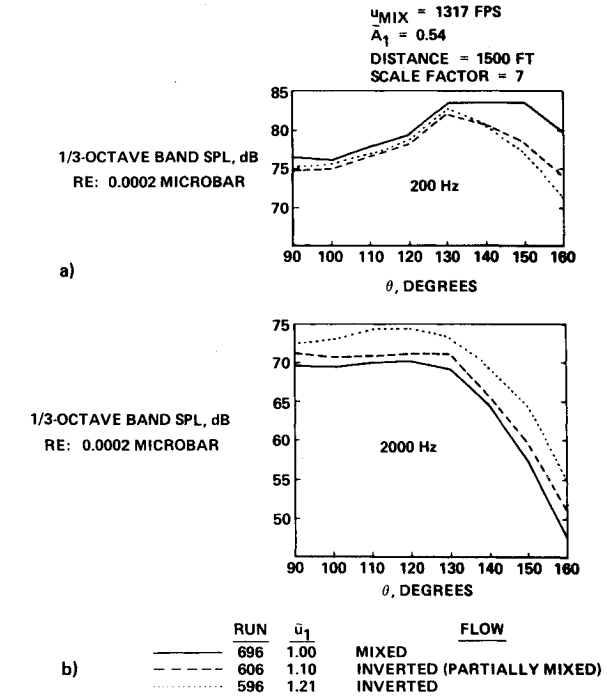

Fig. 12 Effect of inverted flow velocity on SPL directivity.

Examples of the spectral effects of inverted flow velocity ratio are shown in Fig. 14. The corresponding baseline area ratio is 0.54. The changes in the appropriate OASPL shown in this section and the changes in PNL to be shown in the next section can be related directly to these spectra. Profile shaping produces significant changes in spectral content. There is, in general, a high-frequency increase and low-frequency decrease with flow inversion. The extent of these changes is strongly dependent on angle and inverted flow velocity ratio. The effect of profile shaping is strongest at aft angles, although the trends are maintained at all angles. The crossover frequency below which one degree of inversion has

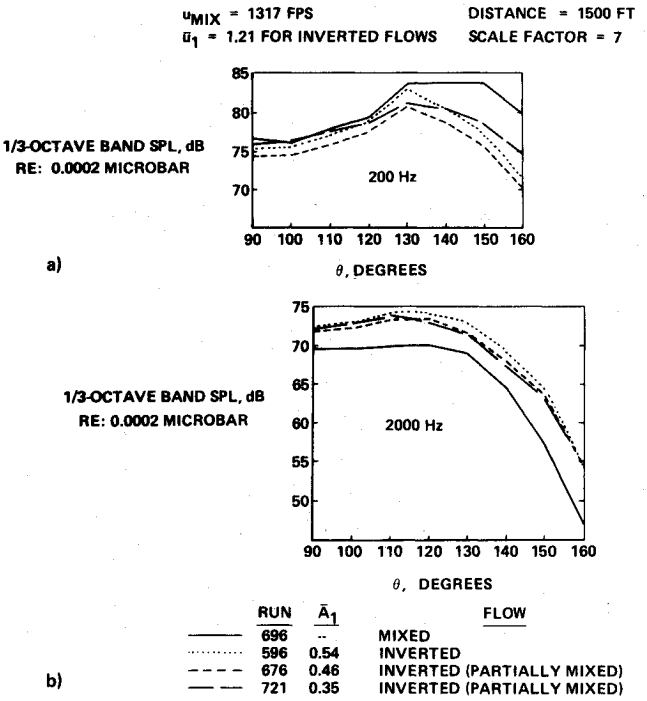

Fig. 13 Effect of inverted flow area ratio on SPL directivity.

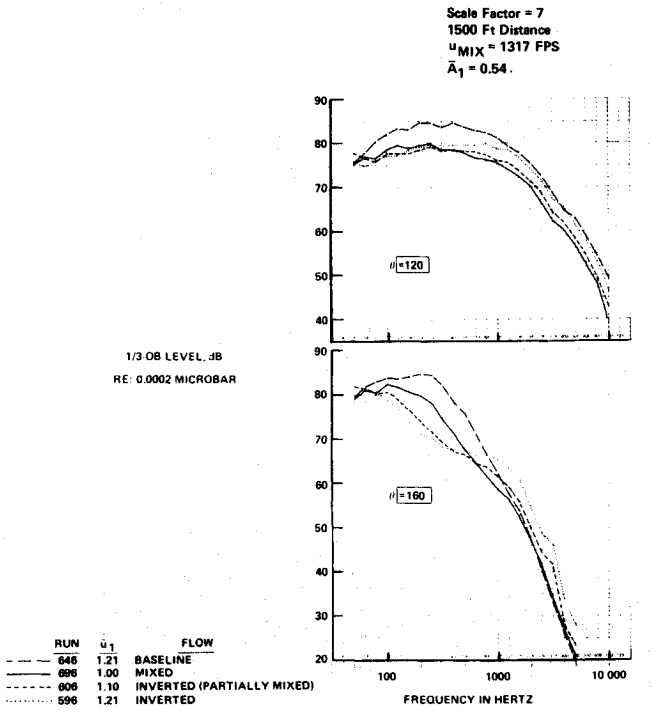

Fig. 14 Effect of profile shaping on spectra.

lower levels than the next becomes progressively lower as the amount of inversion increases.

Perceived Noise Levels

Perceived noise levels were calculated according to the procedure in Ref. 5 for scaled spectra extrapolated to 1500-ft distance at standard day conditions of 77°F and 70% relative humidity. The effect of profile shaping on peak PNL is shown in Fig. 15. Peak PNL reductions of nearly 2 PNdB for inverted-type flows are shown relative to complete mixing, although, in general, the reductions are very small. This is related to the large noy weighting at higher frequencies which are increased with flow inversion. Minimum noise is obtained for inverted flows, but the optimum velocity ratio is nearer 1.05 than 1.15 for most conditions. As with PWL and SPL data, area ratio 0.46 flows consistently produce lower noise levels than area ratio 0.54 or 0.35 flows, and as area ratio decreases, there is an increase in the velocity ratio that produces minimum noise. The fixed area ratio curves for each velocity regime are crossplotted in Fig. 16 to show that inverted profiles produce greater reductions in peak PNL for higher-velocity flow systems.

The effect of inverted flow velocity ratio on PNL directivity is shown in Fig. 17. Noise increases are observed consistently at forward angles, and noise reductions are obtained only at angles aft of 130° for inverted flows relative to complete mixing. The reductions at the aft angles are less than the previously discussed OASPL reductions. However, the aft angle reductions are still meaningful. The acoustic energy at large angles persists for a much longer time during an airplane flyover. This duration effect is accounted for by the parameter PNLW, which is the summing of the PNL's with an angular weighting that is the same as that used implicitly in the computation of airplane flyover effective PNL. It provides a convenient measure of the duration effect between two noise signatures. Reductions in PNL at 150° are more meaningful than at 130°, and some increase in forward angle levels can be acceptable in order to obtain a lower PNLW. PNLW reductions of up to 2 PNdB for inverted-type flows are obtained relative to complete mixing. The same trends are observed for PNLW as for peak PNL except that minimum noise generally is obtained at higher velocity ratios. Inverted profiles produce greater reductions in PNLW for higher-velocity flow systems.

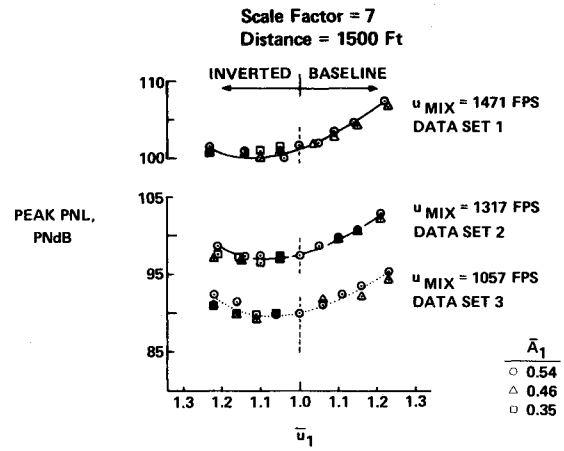

Fig. 15 Effect of profile shaping on peak PNL.

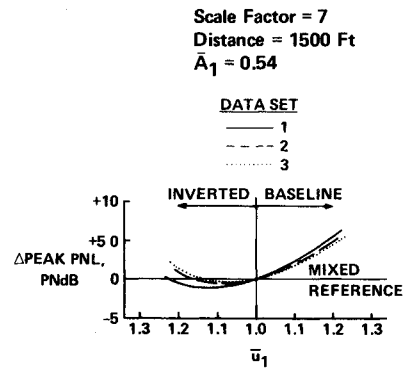

Fig. 16 Peak PNL sensitivity to velocity regime.

Applications

Profile shaping can be applied directly to turbofan engines with long duct nacelle installations and to duct burning turbofan engines. Internal mixing of primary and fan flows can be achieved with long duct nacelles to control the nozzle exit flow profile, and duct burning turbofan engines for advanced supersonic technology (AST) transports can be designed to have a fan exhaust velocity that is substantially higher than the primary exhaust velocity. Internal forced-mixing applications may provide a potential performance improvement because of the associated internal thermodynamic mixing[6] which can help offset the weight penalty of a mixer device. However, the performance improvement for internal mixing must be compromised, since the extent of profile shaping flow inversion obtained is related directly to the control of the primary and secondary flows and subsequent lack of mixing. In addition, circumferential profile distortion generally will result from real mixer designs, and this will change the downstream profile development, which must be accounted for in applying the results of this paper.

Duct burning turbofan engine applications are discussed in Ref. 7. In general, the associated flow systems are at very high velocity regimes which is beneficial for profile shaping as shown in previous sections. Also, four-engine airplanes generally are considered for the AST, which means longer sideline measuring distances. The flow system in the introduction (run 500) provides a PNLW reduction of 1.7 PNdB relative to complete mixing at 1500-ft distance. At 2300-ft distance (corresponding approximately to the 2128-ft sideline FAR 36 certification measuring station) this *reduction increases* to 2.5 PNdB because of the larger effects of atmospheric absorption for the high-frequency content in inverted profile systems. If 20° engine attitude is assumed as perceived for overhead flyovers, the PNLW reduction is increased further to 3.3 PNdB. A reduction of 5 PNdB in peak PNL is presented in Ref. 8 for an inverted flow system with a velocity ratio $\bar{u}_1$ of 1.22 and an area ratio $\bar{A}_1$ of 0.42. It is interesting to note that these conditions correspond very closely with the optimum conditions found in the present experiment.

Indirect applications of profile shaping also are considered. The flow profile in the downstream postmerged region for multielement suppressor nozzles can be controlled by the

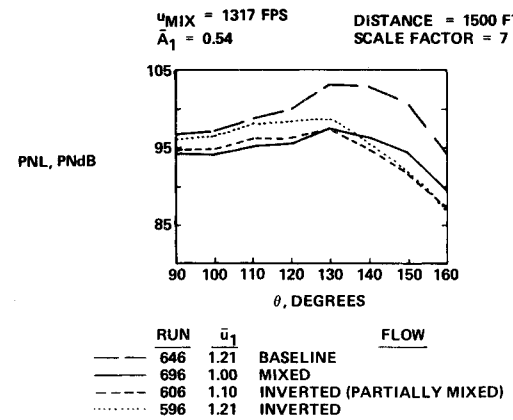

Fig. 17 Effect of inverted flow velocity on PNL directivity.

distribution of the nozzle exit breakup elements as shown in Ref. 1. If the noise signature is dominated by the lower frequencies associated with this postmerged region, profile shaping technology can be applied to optimize the downstream flow profile.

One of the most promising applications of the profile shaping technique is as a low-frequency attenuator which, in conjunction with a lined shroud or similar device to attenuate high-frequency noise, would produce a substantial net reduction. However, if such a system is to work, it is necessary that a substantial portion of the high-frequency noise be generated close enough to the nozzle to react with the lined material. With this in mind, the effect of profile shaping on high-frequency source location was calculated using the analytical flow/noise program developed at Boeing.[8] The relative change in 2000-Hz power level axial distribution for four flow systems which correspond to the systems presented in Fig. 17 was calculated and showed that flow inversion does translate high-frequency source location nearer the nozzle exit. According to these calculations, approximately 35% of the acoustic energy at 2000 Hz is generated within the first diameter downstream of the baseline nozzle exit plane. This compares with 60% for complete mixing, 65% for partially inverted, and 75% for the fully inverted flow systems. More important is the projection that, of the conditions considered, the partially inverted profile ($\bar{u}_j = 1.10$) generates least noise (total energy) downstream of one nozzle diameter and is therefore best suited for nozzle configurations with acoustically lined surfaces immediately downstream of the nozzle exit.

All of the data presented in this paper are static. An important element in profile shaping technology is the behavior of inverted flows with forward speed. There are several active ongoing programs in industry developing the required flight effects technology. In particular, Boeing recently has completed a test program with NASA (Contract No. NAS2-8213) in which a JT8D turbofan engine was tested in the 40- by 80-ft low-speed wind tunnel at the Ames Research Center. An internal forced mixer configuration was tested, and the jet noise suppression was compared between tunnel off and tunnel on. It was found that the peak-to-peak reduction in both PNL and OASPL increased slightly with forward speed.[9] Since the exit profile of the mixer configuration represents a case of partial flow inversion, the increase in suppression with forward speed is significant. This provides the first indication that inverted flow systems may maintain or improve their suppression characteristics in flight. An important follow-on program in the Ames 40- by 80-ft wind tunnel currently is planned to study the flight effects for a JT8D engine with a completely inverted flow system.[10]

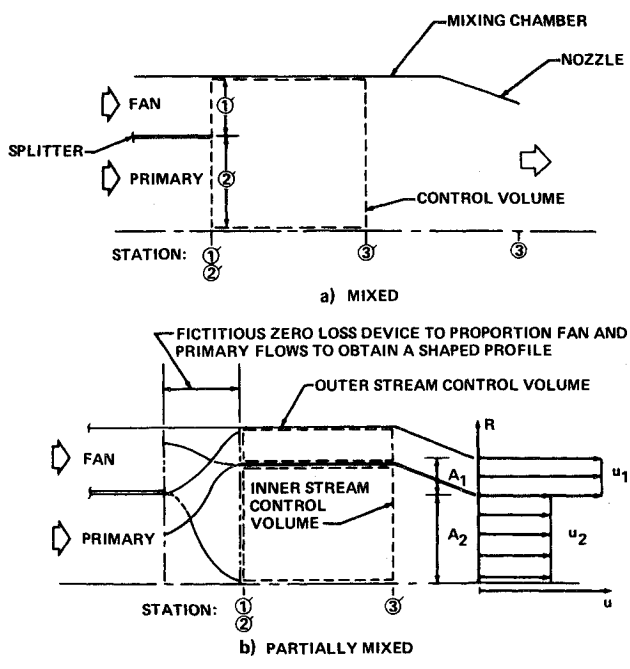

Fig. 18 Control volumes for computing flow properties.

Conclusions

The experimental work reported herein has demonstrated that profile shaping can be used to obtain jet noise reductions beyond complete mixing for a conventional turbofan flow system. The following results were obtained for variations in exit profile under test conditions of approximately constant total system properties (mass flow, energy, and momentum):

1) Inverted velocity profiles produce acoustic effects similar to multielement suppressor nozzles, i.e., low frequencies are reduced and high frequencies are increased. These spectral effects can be used to obtain a balanced noise signature in terms of constant duration weighted PNL directivity and noy spectra. The acoustic changes are consistent with the changes in downstream profile development.

2) Maximum noise reductions obtained for the flow systems in this test are about 3 dB in PWL, 4 dB in peak OASPL, 2 PNdB in peak PNL, and 2 PNdB in PNLW (1500-ft distance) relative to complete mixing.

3) In general, minimum noise is obtained for inverted flows with a velocity ratio between 1.05 and 1.15 (partial mixing). Area ratio 0.46 flows consistently have lower noise levels than area ratio 0.54 and 0.35 flows, which suggests an optimum area ratio as well as velocity ratio for minimum noise. As area ratio decreases, there is an increase in the velocity ratio that produces minimum noise.

4) Greatest noise reductions are obtained at aft angles for inverted flows relative to complete mixing. Increases in noise can occur at forward angles (90° to 130°).

5) Inverted profiles produce greater noise reductions for higher-velocity flow systems (throttle effect).

6) Profile shaping can be applied directly to turbofan engines with long duct nacelle installations (internal forced mixing) and to duct burning turbofan engines (cycle design). Duct burning turbofan engine applications have significant potential because the associated flow systems are at very high velocity regimes. Indirect applications of the profile shaping technique include: a) optimizing the downstream postmerged region of a multielement suppressor nozzle by controlling the distribution of the nozzle exit breakup elements, and b) using profile shaping for low-frequency reduction in conjunction with a lined shroud or similar device to attenuate the high-frequency noise.

7) An important element in profile shaping technology is the behavior of inverted flows with forward speed. Two related programs which address this problem are discussed.

Appendix

Computation of Fully Mixed Reference Conditions

Mixed flow properties were computed following a procedure reported by Kennedy.[11] One-dimensional conservation equations of mass, momentum, and energy are written for the control volume shown in Fig. 18a. Using the equation of state to eliminate density from the continuity, momentum, and energy equations, these equations then are rearranged to give an algebraic relation for $M_{3'}$. Other properties at station 3′ are solved by substitution of $M_{3'}$ back into the original conservation equations. The reference fully mixed nozzle exit conditions then are obtained by expanding the station 3′ flow through the nozzle to ambient pressure. It should be noted that, in general, a total pressure loss caused by the mixing process occurs. This is important, as it requires an increase in nozzle exit area to obtain a "match" with the reference nozzle and no mixer. A "shaped" nozzle exit velocity profile implies incomplete mixing. Thus, the required

nozzle exit area for a shaped velocity profile will not be equal to either the fully mixed or the reference nozzle exit areas.

Computation of Partially Mixed Flow Properties

In the present experiment, circumferential mixing was assumed to be complete at the nozzle exit plane. Coannular nozzles were used to simulate a radial shaping of the nozzle exit velocity profile. In the simulation of various partially mixed or shaped nozzle exit velocity profiles, one wishes to specify A_1 and u_1, compute A_2 and u_2 and the total pressures and temperatures, which must be set in the inner and outer streams of the coannular nozzles. Fan and primary flow properties for the engine cycle being simulated are assumed known.

One approach to computing these quantities is to make use of a fictitious mixing and proportioning device as shown in Fig. 18b. In this approach, the fictitious device is used to transfer various proportions of the fan and primary streams to inner and outer mixing chambers as shown in the figure. Fully mixed and ideally expanded flow properties for the inner and outer streams are computed using the procedure for computing the fully mixed reference conditions. The total pressures and temperatures computed at station 3′ for the inner and outer streams are the conditions which would be set in the inner and outer streams of the coannular nozzles of the experiment. In practice, a rather complex iteration was required to determine the right "mix" of fan and primary flow to achieve the desired shaped profile.

In order to simplify the problem of computing the desired quantities, a Crocco enthalpy distribution,[12] was used to relate total temperature and velocity at the nozzle exit plane. Following Crocco,

$$T_t = au + b$$

where a and b are constants to be determined from known boundary conditions. If one requires that

$$T_t = T_{t_{\text{pri}}} \text{ when } u = u_{\text{pri}}$$

and

$$T_t = T_{t_{\text{sec}}} \text{ when } u = u_{\text{sec}}$$

Then,

$$T_t = \left(\frac{T_{t_{\text{pri}}} - T_{t_{\text{sec}}}}{u_{\text{pri}} - u_{\text{sec}}}\right) u + \frac{u_{\text{pri}} T_{t_{\text{sec}}} - u_{\text{sec}} T_{t_{\text{pri}}}}{u_{\text{pri}} - u_{\text{sec}}}$$

Thus, given u_1, the Crocco relationship implies a T_{t_1}. The compressible Bernoulli equation yields P_{t_1}, and a mass-flow relation gives M_1. M_2 then is computed from continuity, T_{t_2} from an energy balance, and u_2 from the Crocco relationship. The Crocco enthalpy relationship between total temperature and velocity was compared with that computed from the one-dimensional relationships for complete mixing in the inner and outer streams and excellent agreement was obtained.

References

[1] Thornock, R. L. and Atvars, J., "Thrust and Acoustic Performance of the NSC-119C, an Advanced SST Type Noise Suppressor," Boeing Document D6-41990, Oct. 1974.

[2] MacGregor, G. R. and Simcox, C. D., "The Location of Acoustic Sources in Jet Flows by Means of the 'Wall Isolation' Technique," AIAA Paper 73-1041, Seattle, Wash., Oct. 15-17, 1973.

[3] Society of Automotive Engineers, Inc., "Standard Values of Atmospheric Absorption as a Function of Temperature and Humidity for Use in Evaluating Aircraft Flyover Noise," ARP 866, Aug. 1964.

[4] Lu, H. Y., "Multiannular Axisymmetric Jet Flow Prediction Using a Two-Equation Model of Turbulence," Boeing Document D6-42606, Sept. 1975.

[5] Society of Automotive Engineers, Inc., "Definitions and Procedures for Computing the Perceived Noise Level of Aircraft Noise," ARP 865, Oct. 1964.

[6] Hartmann, A., "Theoretical and Experimental Investigation of Fanengines with Mixing; Optimal Layout of Fanengines With and Without Mixing," AIAA Paper 67-416, Washington, D. C., July 17-21, 1967.

[7] Packman, A. B., Kozlowski, H., and Guiterrez, O., "Jet Noise Characteristics of Unsuppressed Duct Burning Turbofan Exhaust System," AIAA Paper 76-149, Washington, D. C., Jan. 26-28, 1976.

[8] Berman, C. H., Jaeck, C. L., and Lu, H. Y., "Analytical Prediction of Jet Noise Generation," Boeing Document D6-40614TN, June 1974.

[9] Strout, F. G., "Flight Effects on Noise Generated by the JT8D-17 Engine in a Quiet Nacelle and a Conventional Nacelle as Measured in the NASA-Ames 40- × 80-Foot Wind Tunnel," NASA CR-137797, Jan. 1976.

[10] Strout, F. G., "Noise Measurement in the 40- by 80-Foot Wind Tunnel of JT8D Engine with Primary/Fan Flow Inverter," Boeing Document D6-42984-1, May 1976.

[11] Kennedy, E. D., "Mixing of Compressible Fluids," *Journal of Applied Mechanics, Transactions of ASME, Ser. E*, Vol. 83, Sept. 1961, pp. 335-338.

[12] Shapiro, A. H., *The Dynamics and Thermodynamics of Compressible Fluid Flow*, Vol. II, Ronald Press, New York, 1954, pp. 1045-1046.